AD NUMBER

AD868160

NEW LIMITATION CHANGE

TO

Approved for public release, distribution unlimited

FROM

Distribution authorized to U.S. Gov't. agencies and their contractors; Administrative/Operational Use; APR 1970. Other requests shall be referred to Commander, Naval Undersea Research and Development Center, San Diego, CA 92132.

AUTHORITY

USNURDC ltr, 15 Sep 1971

NUC TP 171

NUC
TECHNICAL PUBLICATION

DILUTION IN A TURBULENT BOUNDARY LAYER WITH POLYMERIC FRICTION REDUCTION

By
A. G. Fabula and T. J. Burns
Ocean Technology Department

April 1970

NAVAL UNDERSEA RESEARCH
AND DEVELOPMENT CENTER

AN ACTIVITY OF THE NAVAL MATERIAL COMMAND

CHARLES B. BISHOP, Capt., USN
Commander

Wm. B. McLEAN, Ph.D.
Technical Director

The reduction of hydrodynamic drag is of continuing interest to the Navy. The use of long-chain polymer additives appears to be a practical method for reducing skin friction in turbulent boundary-layer flow. It has been under investigation at this Center since 1961.

The work reported here concerns dilution by turbulent mixing of a polymer solution injected into a turbulent boundary layer. The mixing affects the required polymer supply rate and is therefore of importance in planning friction reduction systems. The work was done between October 1968 and March 1969 under Naval Ordnance Systems Command Task No. ORD-054-000/200-1/R 109-01-03. T. E. Peirce, Ph.D., was the NOSC project engineer.

This report was reviewed for technical adequacy by H. P. Bakewell, Jr., Ph.D., of the Navy Underwater Sound Laboratory. Gratitude is expressed to D. M. Nelson of this Center for helpful discussion and to Prof. J. M. Wetzel of the St. Anthony Falls Hydraulic Laboratory, University of Minnesota, for the preliminary experimental data.

Most of the material was presented as a paper at the American Institute of Aeronautics and Astronautics 2nd Advanced Marine Vehicles and Propulsion Meeting in Seattle, 21 to 23 May 1969.

Released by
J. H. GREEN, Head
Applied Science Division
13 March 1970

Under authority of
D. A. KUNZ, Head
Ocean Technology
Department

PROBLEM

Predict the mean concentration distribution of polymer far downstream of the injection of a polymer solution into a two-dimensional, constant-pressure turbulent boundary layer on a flat plate.

RESULTS

The available experimental data and empirical relations for the mixing of a passive scalar quantity, such as smoke or dye after injection into a turbulent boundary layer, appear to be consistent with the outer-layer similarity relations for high Reynolds numbers. The final-zone similarity laws of mixing—which relate mean concentrations, free-stream speed, boundary-layer thickness, and wall shear stress—are developed within the framework of equilibrium boundary-layer flow, assuming the velocity-defect law of Coles and using some experimental results of Poreh and Cermak, Fiedler and Head, and Kibens. The analogy of polymeric friction reduction to a "negative roughness" implies that the polymer can be considered to be a passive scalar outside the thin inner layer, so that the major mixing process is unchanged. The analogy is expected to be valid in some practical ranges of concentration and wall shear stress whose limits must be determined experimentally.

The preliminary results of mixing experiments in an open-channel boundary layer, for injection of dyed water or dyed polymer solution, appear to be consistent with the predictions based on the negative roughness analogy.

RECOMMENDATIONS

The final-zone similarity relations for mixing developed here should be tested by further experiments in nearly constant-pressure flows, with attention to truly two-dimensional conditions. The goal should be to determine the ranges of polymer concentration, wall shear stresses, and slot distances for which the relations are valid. The theoretical predictions of mixing and friction reduction should be combined to predict polymer supply rates and friction reduction for injection systems. In comparing such predictions with experiments, attention must be given to the possible importance of the earlier mixing zones and the concentration fluctuations about the mean, which are not considered in this work.

CONTENTS

NOMENCLATURE

B Constant in logarithmic law of the wall: $B = B_0 + \Delta B$

B_0 Smooth-wall value of B in Newtonian fluids

c Polymer concentration in ppm by weight

c_f $2\tau_w/\rho U^2$

c_i Value of c in injection-slot fluid

c_Q Volume-flux average value of c in the boundary layer: $Q_i c_i/Q$

c_t Volume-flux average value of c in the turbulent fluid: $Q_i c_i/Q_t$

$\bar{c}$ Time average value of c at a point

$\bar{c}^t$ Turbulent conditional average value of c at a point

$\bar{c}_w$ Wall value of $\bar{c}$

G Equilibrium profile parameter: $\int_0^\infty [(U-u)/u_\tau]^2\, d\eta \Big/ \int_0^\infty (U-\bar{u})/u_\tau d\eta$

G_1 Clauser wake function

H Profile shape factor: $H \triangleq \delta^*/\theta$

I Detector function: 1 in turbulent flow; 0 in irrotational flow

k Von Karman "universal" constant; $k \approx 0.41$

$\dot{m}$ Polymer solution mass injection rate per unit span

Q Volume flux of boundary-layer fluid per unit span

Q_i Volume flux of polymer solution per unit span

Q_t Volume flux of turbulent fluid per unit span

t Time

u x-component of the velocity vector

u_τ Local value of the friction velocity: $\sqrt{\tau_w/\rho}$

$\bar{u}$ Time average value of u at a point

$\bar{u}^t$ Turbulent conditional average value of u at a point

U Free-stream speed

$w(\eta)$ Coles' wake function

x, y, z Rectangular coordinates; x measured along surface in flow direction; y normal distance from surface; z spanwise position

$\overline{Y}$ Parameter in the γ distribution

γ Turbulence intermittency function: $\bar{I}$

δ Boundary-layer thickness at which $\bar{u} = 0.99U$

δ_{C1} Boundary-layer thickness used by Clauser

δ_π Boundary-layer thickness in Coles' law of the wake

δ^* Boundary-layer displacement thickness: $(1/U)\int_0^\infty (U - \bar{u})\,dy$

ΔB Change in B with wall roughness or friction reduction

η y/δ_π

θ Boundary-layer momentum thickness: $(1/U)^2 \int_0^\infty \bar{u}(U - \bar{u})\,dy$

λ Value of y at which $\bar{c}/\bar{c}_w = 0.5$

ν Fluid kinematic viscosity

Π Profile parameter in Coles' law of the wake

ρ Water (or polymer solution) density, a constant

σ Parameter in the γ distribution

τ_w Local wall shear stress

Note: In the cases of $\bar{c}$, $\bar{c}_w$, $\bar{u}$, $\overline{uc}$, $\bar{I}$, $\overline{Iu}$, and $\overline{Iuc}$, the overbar indicates the time-average value at a point in space ($\bar{c}^t$, $\overline{Y}$, and $\bar{u}^t$ are exceptions, which are explained above).

INTRODUCTION

The hydrodynamic frictional drag of a marine vessel, as is well known, can be reduced by injecting a solution of any of various long-chain polymers into the boundary layer on the vessel's hull (Ref. 1 and 2). The polymer solution is greatly diluted by turbulent mixing in the boundary layer. The resultant mean concentrations near the hull surface along most of the vessel's length should be close to certain optimum values if the maximum friction reduction is to be obtained for the minimum expenditure of polymer. Thus, the prediction of boundary-layer mixing becomes important to the evaluation of the feasibility of drag-reduction applications.

Until recently, estimates of dilution were made with what might be called a perfect-mixing model. The gradient in mean concentration across the boundary layer was neglected, and the local uniform concentration at each station was assigned according to the boundary-layer volume flux at that station and the polymer mass conservation equation. In the earliest work, that volume flux was estimated simply by integrating the mean velocity profile from the wall out to a conventional definition of boundary-layer thickness; any changes in velocity profile and thickness due to the polymer solution were ignored. Later, the method of estimation was improved by considering the reduction of boundary-layer thickness. In the present work, major improvements are made by considering the intermittency of turbulence and polymer concentration, the profile of mean concentration, and the polymer effects on the boundary-layer mean velocity profile.

Figure 1, reproduced from Ref. 3, illustrates the intermittency of a turbulent boundary layer in its outer part. The smoke-filled boundary layer was illuminated through a narrow slit. Fiedler and Head (Ref. 3) concluded that "smoke-filled and smoke-free regions can be identified with regions of turbulent and non-turbulent flow." This intermittency must be considered in a realistic model of boundary-layer mixing.

Real understanding of the mechanics of turbulent boundary layers is so fragmentary that idealized models of behavior must be relied on. For example, "eddy viscosity" models liken the turbulent momentum transfer by random eddy motion to the viscous transfer in laminar flow by molecular agitation. "Similarity" models reduce the number of variables that have to be considered. Usually, such models are accurate only within the range of the experiments from which the similarity laws are deduced. In the case of turbulent boundary layers in Newtonian fluids, a well-developed similarity analysis is based on the two-layer concept (Ref. 4). For large boundary-layer thickness Reynolds numbers, such as those that occur on marine

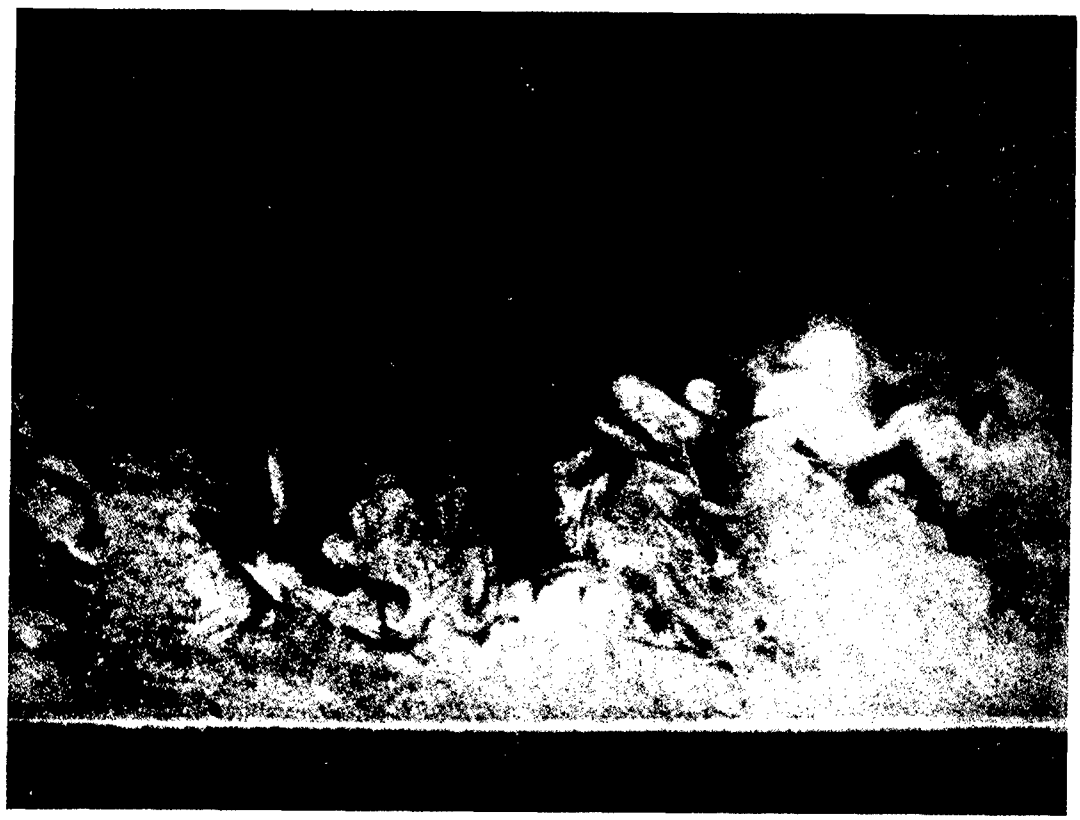

FIG. 1. Smoke in a Turbulent Boundary Layer (from Ref. 3).

vessels, the two-layer model is particularly useful since the velocity-defect similarity law of the outer layer can be used across the entire boundary layer with a good degree of accuracy.

It is particularly simple to incorporate the effects of friction reduction into boundary-layer development calculations if it is assumed that the important polymer effects are confined to the inner layer (the so-called negative roughness analogy). This assumption should be valid for some practical range of operation, and several analyses of turbulent boundary-layer development in polymer solutions have been based on it (Ref. 2, 5 and 6). In the present work, this approach is extended to obtain the similarity relation for the two-dimensional, far-downstream mixing of any passive scalar quantity injected into a boundary layer with friction reduction. Since that relation is an outer-layer law, it is reasonable to expect that it also applies to the far-downstream mixing of injected polymer solution, in accordance with the negative roughness analogy.

The interest in predicting the boundary-layer mixing is a very practical one, since the effectiveness of a polymer solution in reducing friction depends mainly upon its concentration and the wall shear stress. However, experience suggests that

the local friction-reduction effectiveness of a boundary-layer diluted solution of a given mean concentration may be much less than that of a homogeneous solution of the same concentration. Such behavior may be expected if most of the polymer contributing to the local mean concentration is in the form of blobs of small volume-fraction but very high concentration.

Thus, the limitations of the present results must be borne in mind when they are combined with boundary-layer theory to predict the performance of injection systems. In particular, the present work predicts only the far-downstream time-average concentrations and does not predict the intensity of the concentration fluctuations about the mean. Therefore, unanswered questions include how close to an injection slot these relations are useful, and where and how the concentration fluctuations must be considered.

BOUNDARY-LAYER MIXING IN NEWTONIAN FLUIDS

In the two-dimensional, flat-plate, turbulent boundary layer, any quantity such as the instantaneous local concentration of polymer, c, will be a function of x (distance from the leading edge), y (height above the wall), z (spanwise position) and time t. Thus $c = c(x, y, z, t)$, but the time average is independent of z—i.e., $\bar{c} = \bar{c}(x, y)$—when the injection is uniform across the span.

Let $\dot{m}$ be the steady rate of mass discharge per unit span of polymer solution, and let c_i be the polymer concentration (with c_i and c in ppm by weight) in the discharged solution. For all concentrations of interest, the fluid density can be taken as that of the water, ρ (in grams/cm^3). Thus, if $\dot{m}$ is in gram/cm sec, the polymer mass discharge rate per unit span is $10^{-6}\,\dot{m}c_i$ gram/cm sec and the solution volume discharge per unit span is $Q_i = \dot{m}/\rho$ cm^2/sec.

If the x component of the instantaneous velocity at a point is $u = u(x, y, z, t)$, the conservation equation for the polymer mass is

$$Q_i c_i = \overline{\int_0^\infty u(x, y, z, t)c(z, y, z, t)\,dy}$$

because of the uniformity of fluid density. The overbar indicates the time average value which must be independent of z. Interchanging the order of averaging and integration is clearly permissible, so that

$$Q_i c_i = \int_0^\infty \overline{uc}(x, y)\,dy \qquad (1)$$

Fiedler and Head (Ref. 3) studied the far-downstream turbulent mixing of smoke injected into a wind-tunnel boundary layer and found that the smoke was essentially confined to the turbulent fluid and vice versa. The same description is expected to be valid for polymer molecules in water, because molecular diffusion of polymer molecules across the intermittency interface is expected to be negligible. Thus if $I(x, y, z, t)$ is a turbulence detector signal (generated, for example, by a vorticity probe) that is 1 when the flow at a point is turbulent and 0 when it is not, then $c(x, y, z, t)$ can be replaced by $c(x, y, z, t)I(x, y, z, t)$. Hence, $\overline{uc}$ in Eq. 1 can be replaced by $\overline{Iuc} = \gamma \overline{uc}^t$ where $\gamma \triangleq \bar{I}$ is the turbulence intermittency function and $\overline{uc}^t$ is the turbulent-conditional average value of uc at a point. Equation 1 now becomes

$$Q_i c_i = \int_0^\infty \gamma \overline{uc}^t \, dy \tag{2}$$

The similarity laws for $\overline{uc}^t$ have not been studied either experimentally or theoretically. However, it can be expected that $\overline{uc}^t$ will be nearly equal to $\bar{u}^t \, \bar{c}^t$ if the fluctuations of u and c in the turbulent fluid are small relative to their respective means, $\bar{u}^t$ and $\bar{c}^t$. Thus, considering only the turbulent fluid, let $u = \bar{u}^t + u'$, where $\overline{u'}^t = 0$ and $c = \bar{c}^t + c'$, where $\overline{c'}^t = 0$ so that

$$\overline{uc}^t = \bar{u}^t \bar{c}^t + \overline{u'c'}^t = \bar{u}^t \, \bar{c}^t \left[1 + \frac{\overline{u'c'}^t}{(\overline{u'^2}^t \, \overline{c'^2}^t)^{1/2}} \frac{(\overline{u'^2}^t \, \overline{c'^2}^t)^{1/2}}{\bar{u}^t \, \bar{c}^t} \right]$$

Even if u' and c' were "perfectly correlated," i.e., if $|\overline{u'c'}^t| = (\overline{u'^2}^t \, \overline{c'^2}^t)^{1/2}$, and if the relative rms amplitudes of u' and c' were each about 0.25, the error in the approximation $\overline{uc}^t \approx \bar{u}^t \, \bar{c}^t$ would be only about 6%. Thus the approximation seems acceptable and with it, Eq. 2 gives (since $\gamma \bar{c}^t = \bar{c}$)

$$Q_i c_i = \int_0^\infty \bar{u}^t \, \bar{c} \, dy \tag{3}$$

The flows considered are now further restricted in order to make use of the similarity laws of "equilibrium boundary layers" (Ref. 4, 7) for large Reynolds numbers. This makes it possible to approximate the $\bar{u}$ distribution throughout the boundary layer by using the velocity-defect similarity law of Coles (Ref. 8):

$$(U - \bar{u})/u_\tau = -(1/k) \ln \eta + (\Pi/k)[2 - w(\eta)] \tag{4}$$

where Π is a constant in a given type of equilibrium boundary layer; $\eta \triangleq y/\delta_\pi$; δ_π is the definition of boundary-layer thickness associated with Coles' law (with subscript π to distinguish it from δ corresponding to y for $\bar{u}/U = 0.99$); k is the von Karman "universal" constant, about 0.41, and believed to be unchanged with friction reduction caused by dilute polymer solutions; and $w(\eta)$ is given by a tabulated function (Ref. 8) or by $2 \sin^2(\pi\eta/2)$.

In particular, the work is restricted to the constant-pressure type of equilibrium boundary layer, corresponding to that on a flat plate at zero incidence to a uniform free stream. It is thus possible to make use of recent experimental measurements which suggest the similarity laws for $\bar{u}^t$ and $\bar{c}$.

Kibens (Ref. 9) measured $\bar{u}^t$ in a nearly constant-pressure flow. His results for $\bar{u}^t$, $\bar{u}$, and γ are reproduced in Fig. 2, where it can be seen that $\bar{u}^t$ is at most about 2% less than $\bar{u}$ and then only where γ (and hence $\bar{c}$) is nearly zero. This result is quite different from the suggestion of Sarnecki (Ref. 10) that $\bar{u}^t$ should satisfy the logarithmic law of the wall for $\bar{u}$ (cf. Fig. 2). With the approximation $\bar{u}^t = \bar{u}$ in Eq. 3,

$$Q_i c_i = \int_0^\infty \bar{u}\,\bar{c}\,dy \tag{5}$$

Poreh and Cermak (Ref. 11) studied the two-dimensional turbulent mixing of ammonia gas from a wall line source under a wind-tunnel boundary layer. They found four zones of development of the mean concentration profile, as sketched in Fig. 3. In the fourth and final zone, they found that the normalized distribution $\bar{c}(x, y)/\bar{c}_w(x)$, within the experimental scatter, was a function of y/λ alone, where λ is defined such that $\bar{c}/\bar{c}_w = 0.5$ at $y = \lambda$. They also concluded that $\lambda/\delta = 0.64$ in the final zone. Based on an eddy-diffusion analysis, Morkovin (Ref. 12) described their collected data for $\bar{c}/\bar{c}_w$ versus y/λ in that final zone with an expression convenient for the purposes of this report:

$$\bar{c}/\bar{c}_w = \exp[-0.693(y/\lambda)^{2.15}] \tag{6}$$

For the U/u_τ range of the experiments of Ref. 11, it can be shown[1] that $\delta \approx 0.9\delta_\pi$, so that, assuming that λ/δ_π is constant and independent of U/u_τ, $\lambda/\delta_\pi \approx 0.58$ is the final zone law, and Eq. 6 becomes

$$\bar{c}/\bar{c}_w = \exp[-2.27(y/\delta_\pi)^{2.15}] \tag{7}$$

In order to use Eq. 4 and 7 in Eq. 5, the latter can be rewritten as

$$Q_i c_i = u_\tau \bar{c}_w \delta_\pi \int_0^\infty [U/u_\tau - (U - \bar{u})/u_\tau]\,\bar{c}/\bar{c}_w\,d\eta$$

or

$$U\delta_\pi \bar{c}_w / Q_i c_i = \left[\int_0^\infty \bar{c}/\bar{c}_w\,d\eta - (u_\tau/U)\int_0^1 (\bar{c}/\bar{c}_w)(U - \bar{u})/u_\tau\,d\eta\right]^{-1}$$

---

[1] The G_1 wake function of Clauser (Ref. 7) leads to a better description of the u profile near $\bar{u}/U = 0.99$ than does $w(\eta)$. Using Eq. 4 and the equivalent expression in terms of $G_1(y/\delta_{Cl})$, where δ_{Cl} is the boundary-layer thickness used by Clauser, it can be shown that $\delta_{Cl}/\delta_\pi \approx 1.08$ if $k = 0.41$. Thus, $\delta/\delta_\pi \approx 1.08\,\delta/\delta_{Cl}$, and δ/δ_{Cl} can be determined as a function of U/u_τ using the velocity-defect law plot for $G_1(y/\delta_{Cl})$.

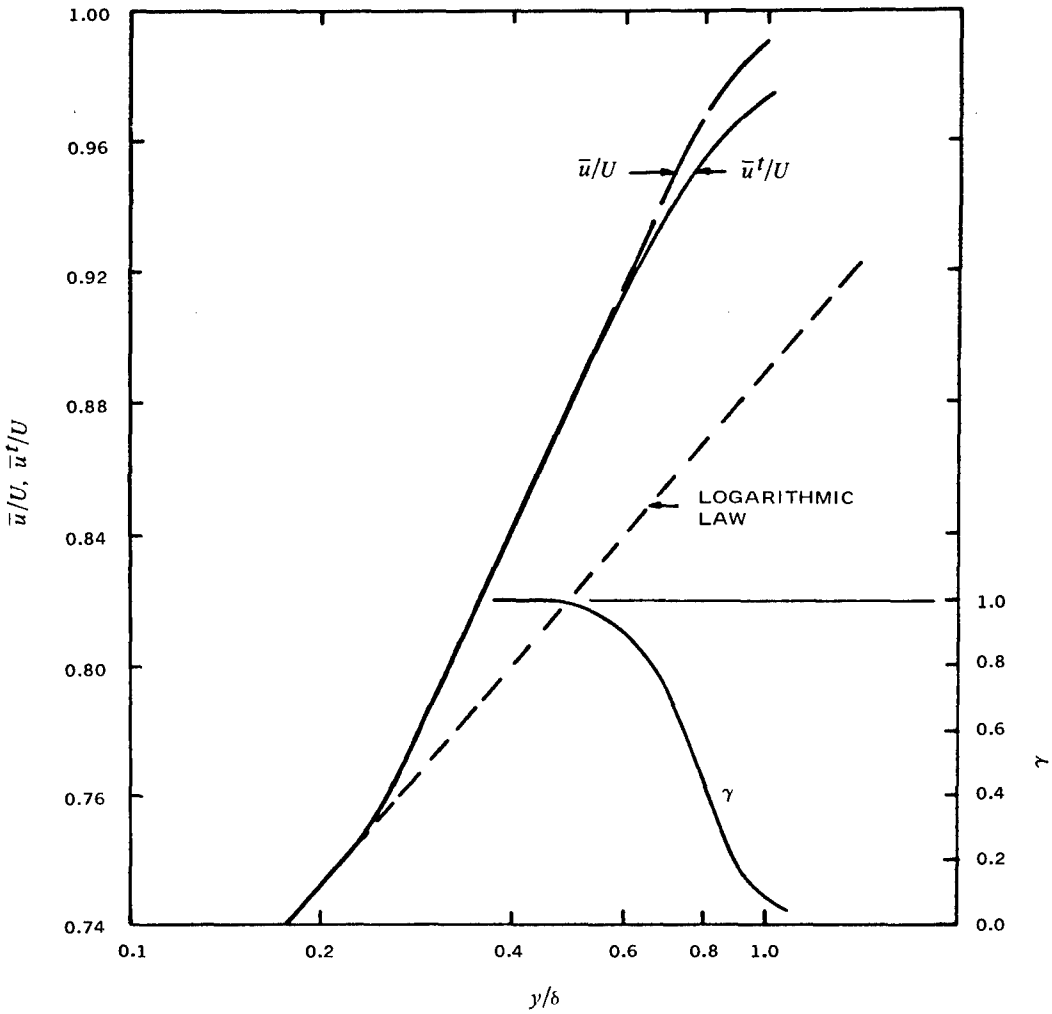

FIG. 2. Experimental Data for $\bar{u}^t/U, \bar{u}/U$, and γ in a Nearly Constant-Pressure Boundary Layer (from Ref. 9).

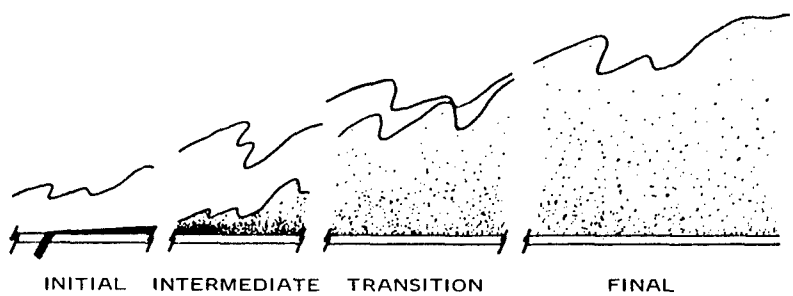

FIG. 3. Mixing Zones Downstream of a Wall Line Source of a Passive Scalar (Ref. 11).

Using Eq. 4 and 7 to evaluate the integrals, while taking $k = 0.41$ and $\Pi = 0.55$ (the value suggested for constant-pressure flow in Ref. 8), the result is

$$U\delta_\pi \bar{c}_w / Q_i c_i = (0.606 - 3.13 u_\tau / U)^{-1} \tag{8}$$

Before comparing this relation with experiment, it is of interest to compare $\bar{c}_w$ according to Eq. 8 with two underestimates. First consider c_t, the boundary-layer volume-flux average value of c, which disregards the concentration profile, so that

$$Q_i c_i = Q_t c_t \tag{9}$$

Since only the turbulent fluid has nonzero c, it is appropriate to make Q_t the turbulent fluid volume flux through the boundary layer:

$$Q_t \triangleq \int_0^\infty \overline{uI}\, dy = \int_0^\infty \gamma \bar{u}^t\, dy$$

Using the approximation $\bar{u}^t = \bar{u}$ in the Q_t integral, Eq. 9 gives

$$Q_i c_i = U\delta_\pi c_t \left[\int_0^\infty \gamma d\eta - (u_\tau / U) \int_0^1 \gamma (U - \bar{u})/u_\tau\, d\eta \right] \tag{10}$$

It is shown in the Appendix that the assumption that $\gamma = \gamma(\eta)$ with the experimental estimate of $\gamma(\eta)$ for constant-pressure flow from Ref. 8 leads to

$$U\delta_\pi c_t / Q_i c_i = (0.825 - 3.68 u_\tau / U)^{-1} \tag{11}$$

Thus $c_t \approx 0.7\bar{c}_w$ for typical values of U/u_τ, so that c_t as an estimate of $\bar{c}_w$ would be typically about 30% low.

The second and more crude estimate for $\bar{c}_w$ is c_Q, which is obtained by replacing Q_t in Eq. 9 by the common measure of volume flux through the boundary layer, Q:

$$Q \triangleq \int_0^U \bar{u}(dy/d\bar{u}) d\bar{u}$$

This estimate neglects both the concentration profile and the intermittency. Using the $\bar{u}$ profile law assumed in this work, the result is

$$U\delta_\pi c_Q / Q_i c_i = (1 - 3.78 u_\tau / U)^{-1}$$

which yields $c_Q \approx 0.6\bar{c}_w$ for the high U/u_τ values of interest, so that c_Q is about 40% low.

Figure 4 shows the plots of Eq. 8 and 11 versus U/u_τ, along with the experimental data of Ref. 11 for $U\delta\bar{c}_w / Q_i c_i$. Since the values of U/u_τ for the experimental

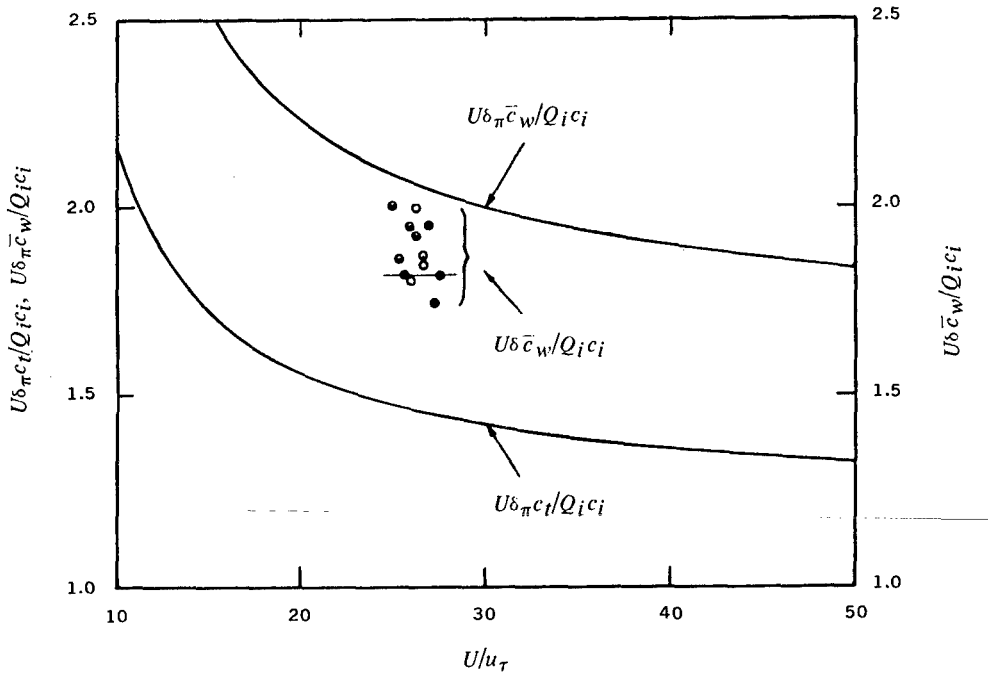

FIG. 4. Predicted Mixing Similarity Laws for $\bar{c}_w$ and c_t Versus U/u_τ (Eq. 8 and 11), Compared With Experimental Data for $U\delta\bar{c}_w/Q_i c_i$ (Ref. 11).

data are not given in Ref. 11, they were estimated by means of the relation of Schulz-Grunow (Ref. 13) for the experimental U, x, and ν values. As previously mentioned, $\delta \approx 0.9\delta_\pi$ in the experimental U/u_τ range, so that the center of gravity of the experimental points would be roughly on the theoretical line for $U\delta_\pi\bar{c}_w/Q_i c_i$ if that correction were made. A best-fit straight line through the data would have a steeper slope than the theoretical curve, but the experimental scatter makes this conflict of little certainty at this time. It is interesting that Poreh and Cermak fitted the line of zero slope shown in Fig. 4 in keeping with their assumption of Eq. 5 with a power-law profile $\bar{u}/U = (y/\delta)^{1/n}$, which implies that $U\delta\bar{c}_w/Q_i c_i$ is constant.

Equations 7 and 8, for $\bar{c}/\bar{c}_w$ and $U\delta_\pi\bar{c}_w/Q_i c_i$, seem to be the best available similarity estimates for the far-downstream mixing of a passive scalar injected uniformly from a line source into a two-dimensional, constant-pressure boundary layer. The generalization of these results to include the case of polymeric friction reduction follows.

THE "NEGATIVE ROUGHNESS" ANALOGY

Wall roughness does not enter into the work discussed above, since wall roughness affects the skin friction but not the velocity-defect similarity law nor the intermittency distribution, $\gamma(y/\delta)$, according to Ref. 14. There is also the expectation[2]

[2] Private communication from J. E. Cermak, University of Colorado.

that wall roughness does not affect the final zone law for $\bar{c}/\bar{c}_w$. It is notable, therefore, that polymeric friction reduction has been likened to a negative roughness on the basis of the following comparison of characteristics:

	Wall Roughness	Polymeric Friction Reduction
τ_w change:	>0	<0
ΔB change:	<0	>0

where τ_w is the wall shear stress ρu_τ^2, and ΔB is the shift of the constant B in the logarithmic law of the wall:

$$u/u_\tau = (1/k)\ln(yu_\tau/\nu) + B;\ B = B_0 + \Delta B \tag{12}$$

where B_0 is the smooth-wall value for Newtonian fluids. Since it is known that the polymer can affect the flow away from the wall (Ref. 15), it is clear that the analogy can be only a partial one. It can be predicted that in many practical cases the lower concentrations away from the wall and the lower Reynolds stresses there render the viscoelastic effects of the polymer unimportant. For such cases, it is reasonable to expect that the velocity-defect law, the intermittency distribution, and the mixing law will be unchanged with polymeric friction reduction since they are unchanged with wall roughness. The similarity relations for $\bar{c}/\bar{c}_w$, λ/δ_π, and $U\delta_\pi\bar{c}_w/Q_i c_i$ should therefore be unchanged with polymeric friction reduction. A test of this expectation is made below.

A COMPARISON WITH EXPERIMENT

A project at the St. Anthony Falls Hydraulic Laboratory (SAFHL) of the University of Minnesota involves the mixing process in a turbulent boundary layer with polymeric friction reduction. The investigation is being made in a 9-foot-wide, open-water channel in which there is a steady, approximately two-dimensional flow of about 1 foot in depth. In order to study mixing with and without friction reduction, dyed polymer solution (Polyox WSR-301) or dyed water is injected through a tangential wall slot extending across the channel near the effective start of the boundary layer. The mean dye concentration at various points in the flow downstream of the slot is determined by sampling the flow through pitot tubes that are also used to determine the mean velocity profile. Two representative profiles of $\bar{u}$ and dye $\bar{c}$ for injection of water and 500-ppm Polyox WSR-301 solution[3] are shown in Fig. 5 and 6. In both cases, the sampling station is 16 feet downstream of the injection slot. The values of Q_i and dye c_i are listed in the figures. It can be shown that 16 feet is far enough for "final-zone" behavior to be expected according to the results of Ref. 11. Since the dye dilution factor at the wall, $c_i/\bar{c}_w$, is about 5/0.06 in the case

[3] Private communication from Prof. J. M. Wetzel, SAFHL.

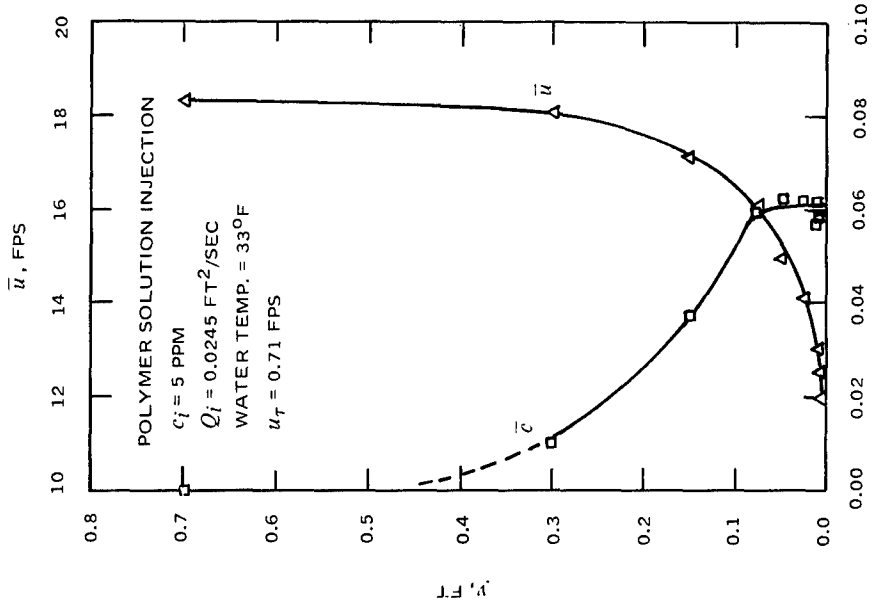

FIG. 6. Preliminary SAFHL Data for $\bar{c}$ and $\bar{u}$ at $x = 16$ ft for Dyed Polymer Solution Injection.

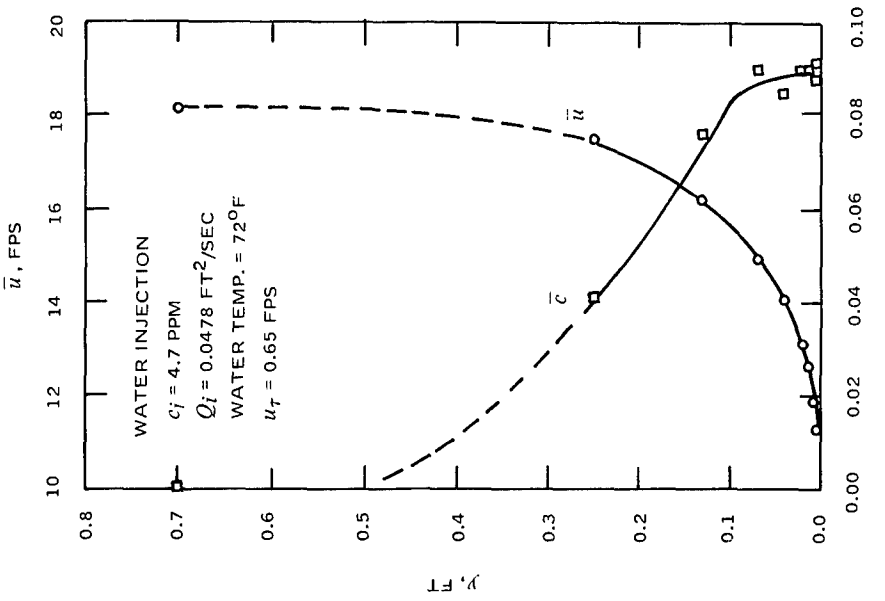

FIG. 5. Preliminary SAFHL Data for $\bar{c}$ and $\bar{u}$ at $x = 16$ ft for Dyed Water Injection.

of polymer-solution injection, the mean polymer-solution concentration at the wall is about (0.06/5) 500 ppm or only 6 ppm. This low value and the moderate wall shear stress (discussed later) suggest that the negative roughness analogy should apply.

Figure 7 shows the plots of y/λ versus $\bar{c}/\bar{c}_w$, based on Fig. 5 and 6, plus the prediction of Eq. 6. The comparison is quite good and supports the expectation of final zone behavior and the negative-roughness analogy.

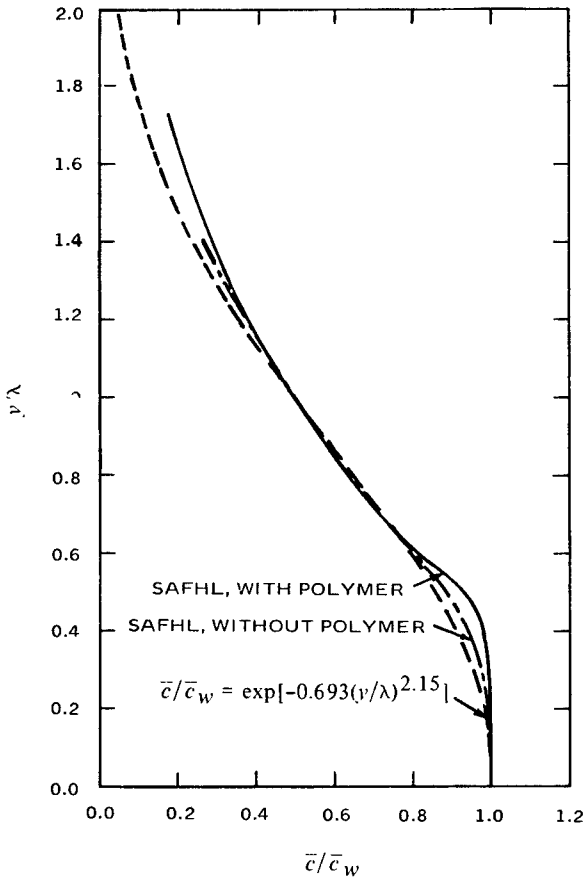

FIG. 7. Profiles of y/λ Versus $\bar{c}/\bar{c}_w$ From Fig. 5 and 6, Compared With the Final Zone Empirical Law.

In order to check on the predictions of $\bar{c}_w$ and λ, u_τ, and δ_π or δ are needed. The values of u_τ listed in Fig. 5 and 6 are SAFHL estimates that were inferred from the velocity profiles by use of the logarithmic law of the wall. These rather uncertain estimates were used in comparing the experimental results for $\bar{c}_w$ and λ with theory. In view of the limited amount of $\bar{u}$ data, δ_π was assigned as follows. Each displacement thickness, δ^*, was first determined from the corresponding $\bar{u}$ profile, using

$$U\delta^* \triangleq \int_0^\infty (U - \bar{u})\, dy \qquad (13)$$

The SAFHL data fairings shown in Fig. 5 and 6 were used in Eq. 13 and were extrapolated to $\bar{u} = 0$ using the logarithmic law of the wall. The resultant δ^* estimates, the corresponding values of $U\delta^*/\nu$ (based on water viscosity at the test temperatures), and the SAFHL estimate of U/u_τ for each injection case are:

	Water	Polymer Solution
δ^*, ft	0.0389	0.0287
$U\delta^*/\nu$	68,500	26,900
U/u_τ	27.9	30.5

The δ_π values were calculated from the δ^* values by means of the relation for δ^*/δ_π from the velocity-defect law of Eq. 4 (for $k = 0.41$ and $\Pi = 0.55$) and Eq. 13:

$$\delta^*/\delta_\pi = (u_\tau/U)(\Pi + 1)/k = 3.78u_\tau/U \tag{14}$$

Before using the δ_π values, a check on the consistency of the U/u_τ and $U\delta^*/\nu$ values can be made by use of the relation between U/u_τ and $U\delta^*/\nu$ for constant-pressure flow of Newtonian fluids. Figure 8 (reproduced in most part from Ref. 4) gives the plot of U/u_τ versus $\log(U\delta^*/\nu)$ for Newtonian constant-pressure flow on a smooth wall. The experimental (aerodynamic) data of two investigations and two

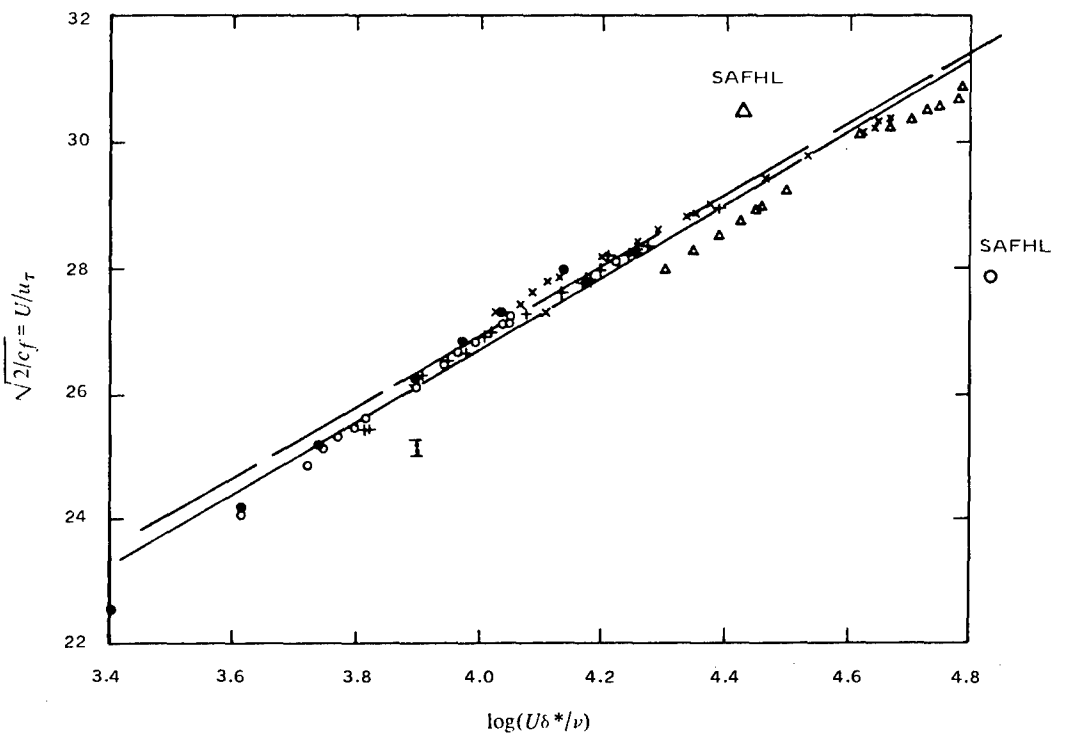

FIG. 8. Comparison of Newtonian-Fluid Relation for U/u_τ Versus $\log(U\delta^*/\nu)$ for Constant-Pressure Flow Over a Smooth Flat Plate (from Ref. 4) With Data Points Based on $\bar{u}$ Plots in Fig. 5 and 6.

semi-theoretical expressions are shown, along with the two SAFHL data points. The solid line (from Ref. 4) corresponds to $U/u_\tau = 5.75 \log(U\delta^*/\nu) + 3.7$. The dashed line is obtained from the matching of the velocity-defect law of Eq. 4 with the logarithmic law of the wall (Eq. 12), giving

$$U/u_\tau = (1/k) \ln(u_\tau \delta_\pi/\nu) + B + 2\Pi/k$$

By use of Eq. 14, this becomes

$$U/u_\tau = (1/k) \ln(U\delta^*/\nu) + B + 2\Pi/k - (1/k) \ln[(\Pi + 1)/k] \qquad (15)$$

The dashed line in Fig. 8 is $U/u_\tau = 5.62 \log(U\delta^*/\nu) + 4.44$ according to Eq. 15 for $k = 0.41$, $\Pi = 0.55$, and the Newtonian fluid, smooth-wall value of B ($B_0 = 5.0$). Both of the semi-theoretical lines are in reasonable agreement with the aerodynamic data, but a lower slope, i.e., a smaller value of $(1/k) \ln 10$, may be needed at the high end of the $U\delta^*/\nu$ range.

The fact that both SAFHL points are outside the spread of the aerodynamic data is not surprising. The low U/u_τ value for the water-injection case (shown by the circle) is reasonable because a ΔB of −3 corresponds to an equivalent sand-grain roughness for the channel bottom of a likely magnitude, according to the Prandtl-Schlichting relation (Ref. 16). However, an overestimate of u_τ could produce the same result for a smooth wall. The high U/u_τ for the polymer-solution injection case (shown by the triangle) implies a ΔB due to the polymer of +5 if the reference friction line passes through the water-injection point, parallel to the smooth-wall line. This ΔB is very low in comparison with the pipe-flow ΔB values found by Goren and Norbury (Ref. 17) for the same polymer type and concentration. If the wall shear stress, ρu_τ^2, for the polymer-solution case is estimated as 300 dyne/cm^2, then the extrapolation of the ΔB versus τ_w data in Ref. 17 according to the Meyer Law, $\Delta B = (a/2) \ln(\tau_w/\tau_{w,\mathrm{crit}})$, implies a ΔB of about 25 for 6 ppm of Polyox WSR-301. The lower ΔB may reflect any of several factors, such as wall roughness, an overestimate of u_τ, a breakdown of Meyer's relation, or differences of solution properties.

Bearing in mind the uncertainty in the u_τ and δ_π estimates, the experimental values of $\bar{c}_w$ and δ can be compared with the predictions of Eq. 8 and $\lambda/\delta_\pi = 0.58$. The experimental profiles in Fig. 5 and 6 and the previously listed δ^* values yield:

	Water	Polymer Solution
$U\delta^*\bar{c}_w/Q_i c_i$	0.28	0.26
λ, ft	0.23	0.18

The values of δ^*/δ_π according to Eq. 14 and the SAFHL estimates of U/u_τ were used to convert these to values of $U\delta_\pi\bar{c}_w/Q_i c_i$ and λ/δ_π. The results are as follows:

	Water	Polymer Solution
δ^*/δ_π	0.136	0.124
$U\delta_\pi \bar{c}_w/Q_i c_i$	2.07	2.10
λ/δ_π	0.81	0.77

These values are shown in Fig. 9 along with the predictions of the scaling relations.

The comparison in Fig. 9 supports the negative-roughness analogy in that the results for water and polymer-solution injection are again quite similar. However, while the $\bar{c}_w$ comparison between prediction and experiment is good, the large percentage of disagreement for λ shows that the $\bar{c}_w$ agreement is partly accidental, since the lower predicted λ values mean a lower predicted flux through the boundary layer. This conflict reflects the fact that the experimental $\bar{u}$ and $\bar{c}$ plots in Fig. 5 and 6 yield values of $\int_0^\infty \bar{u}\,\bar{c}\,dy$ which are 50 to 60% higher than the experimental values of $Q_i c_i$. It would seem that either the flow in the SAFHL channel is significantly three-dimensional or that the approximation of $\overline{uc}$ by $\bar{u}\,\bar{c}$ in the theory is in significant error. The latter case would be the more surprising, since the difficulties of obtaining two-dimensional flow are well known, and, in fact, flow visualization in the SAFHL channel showed that there is an appreciable lateral contraction of the dyed fluid from the slot.

In general, it is more desirable to work with displacement or momentum thickness (δ^* or θ) instead of with δ_π. The predicted scaling relations in terms of δ^*, from Eq. 8 and 14, are

$$U\delta^*\bar{c}_w/Q_i c_i = 3.78\,(0.606U/u_\tau - 3.13)^{-1} \tag{16}$$

$$\lambda/\delta^* = 0.15U/u_\tau \tag{17}$$

Since θ is directly involved in friction reduction work and since its experimental determination is less sensitive to error in $\bar{u}$ near the wall, it is the most desirable thickness parameter. For $k = 0.41$ and $\Pi = 0.55$, use of the velocity-defect law in Eq. 4 across the entire boundary layer yields [from $\theta \triangleq (1/U)^2 \int_0^\infty \bar{u}(U - \bar{u})\,dy$]

$$\theta/\delta^* = 1 - 6.64u_\tau/U \tag{18}$$

Thus the predicted scaling relations in terms of θ are

$$U\theta\bar{c}_w/Q_i c_i = 3.78\,(0.606U/u_\tau - 3.13)^{-1}(1 - 6.64u_\tau/U) \tag{19}$$

$$\lambda/\theta = 0.15U/u_\tau(1 - 6.64u_\tau/U)^{-1} \tag{20}$$

As an example of the use of these predictions, Fig. 10 gives the plots of $\bar{c}$ versus y according to Eq. 19 and 20 for the experimental values of U, Q_i, c_i, U/u_τ, and θ from Fig. 5 and 6. The θ values determined from the experimental $\bar{u}$ plots are listed in Fig. 10; the dashed curves are the experimental fairings in Fig. 5 and 6.

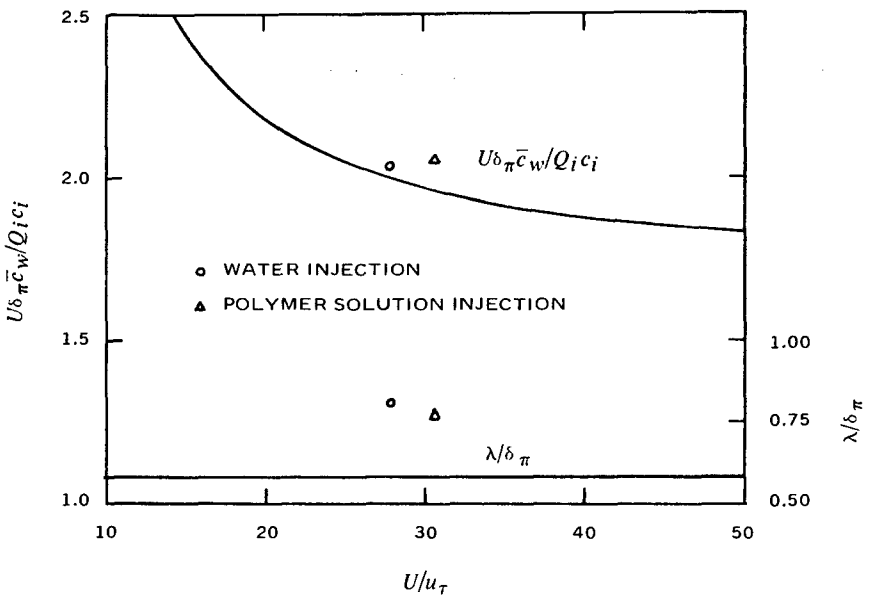

FIG. 9. Comparison of Predicted Law for $U\delta_\pi \bar{c}_w/Q_i c_i$ and λ/δ_π Versus U/u_τ With Data Based on $\bar{c}$ Plots in Fig. 5 and 6.

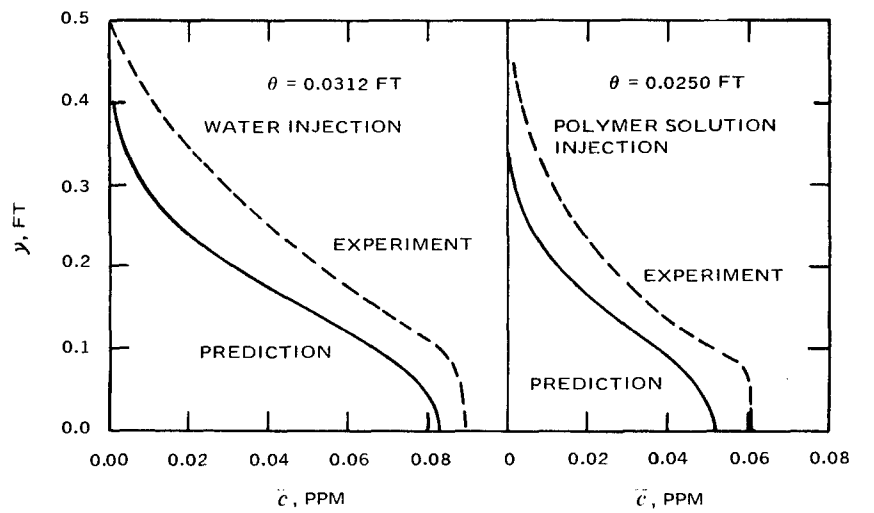

FIG. 10. Comparison of Predicted and Experimental $\bar{c}$ Profiles in the SAFHL Tests, Based on Experimental θ Values.

This dimensional comparison of prediction with experiment shows that there is qualitative agreement of the $\bar{c}$ profiles but a sizable underestimate of $\bar{c}$ all across the profile. This is due, at least partly, to the large experimental difference in the SAFHL results between $Q_i c_i$ and the $\bar{u}\,\bar{c}$ integral, which should be very nearly equal, as far as is known. Thus, if most of the difference is due to three-dimensionality, the quantitative agreement is expected to be better for truly two-dimensional flows.

More extensive comparisons of the predictions of Eq. 19 and 20 with additional preliminary data from SAFHL[4] are given in Fig. 11 and 12. In Fig. 11, eleven experimental values of $\bar{c}_w$ for x = 16 or 40 feet from the injection slot are used in two ways. The unflagged symbols represent experimental values of Q_i; the flagged symbols represent values of Q_i computed from Eq. 5, using the experimental $\bar{u}$ and $\bar{c}$ distributions.[5] This estimated correction for the effects of three-dimensionality makes the experimental points fall roughly as much too low as they fell too high before the correction; thus, the correction is not adequate. The comparison for λ/θ in Fig. 12 is not affected by the Q_i correction. It shows, as was the case in Fig. 9, that the experimental λ values are significantly high, i.e., by about 30% for their center of mass. In view of the small number and the scatter of the data, no significant differences in the comparisons for water versus polymer solution injection, or for x = 40 versus 16 feet, can be inferred from Fig. 11 and 12, despite the two exceptional points in Fig. 12.

The amount of disagreement between the theoretical and the preliminary experimental results cannot be explained at this time. There are many probable causes, but only those on the theoretical side are discussed here. First, the empirical similarity laws assumed in the theory are subject to future refinement. For example, the λ/δ = 0.64 value of Poreh and Cermak for the final zone may be somewhat low, as consideration of Fig. 7 in Ref. 11 seems to suggest. Increasing λ/δ (and hence λ/δ_π) would tend to improve the agreement in both Fig. 11 and 12, since a higher λ means that a lower $\bar{c}_w$ is required by the polymer conservation equation.

It is of interest, therefore, to see what shift in the theoretical relations results from a conceivable increase in λ/δ, e.g., from 0.64 to 0.70. It can be seen that it causes a 9% increase in λ/θ and a decrease in $U\theta\bar{c}_w/Q_i c_i$ of about the same amount. These shifts would move the theoretical curves noticeably toward the centers of mass of the experimental points in Fig. 11 (using the flagged points, of course) and in Fig. 12. Thus, the possibility of an improved estimate for λ/δ_π in the final zone should be kept in mind.

An increase in λ/δ_π would, however, aggravate a questionable feature in the final zone profile of $\bar{c}^t/\bar{c}_w$ which is implied in, but not of direct importance to, the present analysis. Because the scalar concentration in the nonturbulent fluid is everywhere zero, $\bar{c}^t/\bar{c}_w$ must equal $(\bar{c}/\bar{c}_w)/\gamma$. Since both $\bar{c}/\bar{c}_w$ and γ approach zero at the

---

[4] From Dr. Wetzel; see footnote 3, page 9.

[5] Justin McCarthy of Naval Ship Research and Development Center supplied the integrations of $\bar{u}\,\bar{c}$.

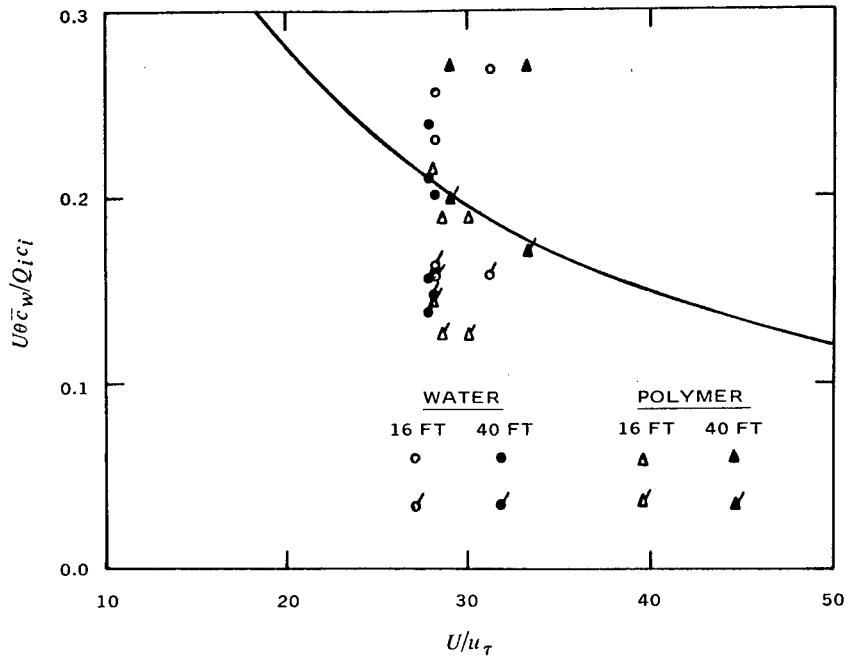

FIG. 11. Comparison of Predicted Law for $U\theta\bar{c}_w/Q_i c_i$ Versus U/u_τ With Preliminary SAFHL Data for Water or Polymer Solution Injection and x = 16 or 40 ft. (For the flagged symbols, Q_i was adjusted to satisfy Eq. 5.)

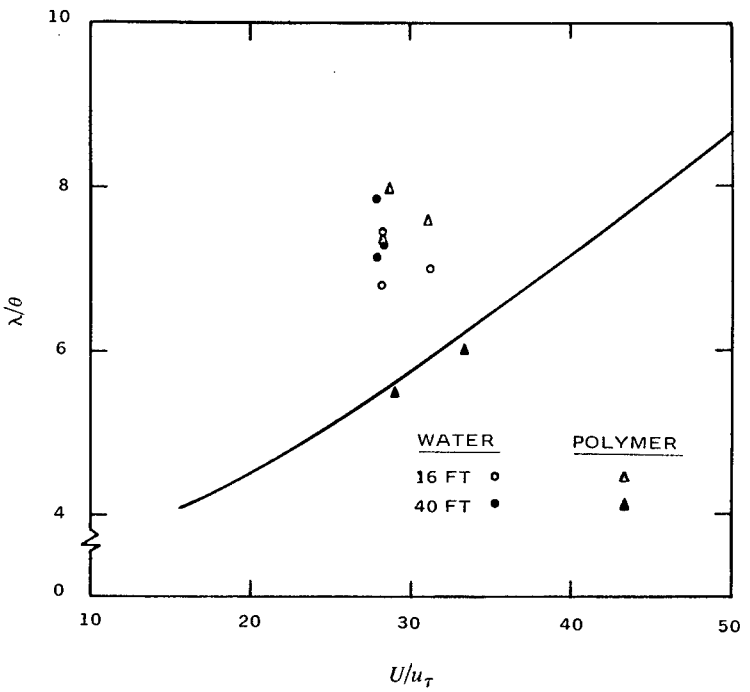

FIG. 12. Comparison of Predicted Law for λ/θ Versus U/u_τ With Preliminary SAFHL Data for Water or Polymer Solution Injection and x = 16 or 40 ft.

edge of the boundary layer, their ratio there is sensitive to error in either part. In particular, the $\bar{c}/\bar{c}_w$ and γ distributions used in this work, which were taken from separate experimental studies, imply that $\bar{c}^t/\bar{c}_w$ dips to about 0.4 at $y/\delta_\pi \approx 0.75$ and then climbs to about 1.0 at $y/\delta_\pi = 1.0$. This reversal seems peculiar, and the conceivable increase in λ/δ from 0.64 to 0.70, as discussed above, would by itself make the reversal more pronounced. Perhaps, however, the cause of the reversal is primarily an overestimate of $\bar{c}/\bar{c}_w$ for larger y/λ by the assumed $\bar{c}/\bar{c}_w$ profile. In fact, inspection of Fig. 1(a) in Ref. 12 suggests that such is the case.

Thus, possible improvements in both final-zone similarity laws, the value of λ/δ_π and the profile of $\bar{c}/\bar{c}_w$ versus y/λ, are of interest. However, since small changes in $\bar{c}/\bar{c}_w$ for $y/\lambda \gtrsim 1.2$ will have little effect on the present prediction, because of the small contribution to the $\bar{u}\,\bar{c}$ integral in that range, the possible correction to λ/δ_π is more likely to be of importance.

SUMMARY

The available experimental data and empirical relations for the far-downstream mixing of a passive scalar injected into a Newtonian-fluid, constant-pressure, flat-plate, turbulent boundary layer appear to be consistent with the outer-layer similarity law of that class of equilibrium flows. Thus, invoking the analogy of polymeric friction reduction to negative roughness, so that the outer-layer mean-velocity similarity (and, presumably, any other important feature of the outer layer) is unaffected by friction reduction, the similarity law of mixing with polymeric friction reduction is predicted to be the same as it is without polymeric friction reduction.

In order to develop the similarity laws within the framework of equilibrium boundary-layer theory, the velocity-defect law of Coles is adopted, along with his definition of boundary thickness (δ_π) and his values for the law-of-the-wake parameter Π of 0.55 for the case of constant-pressure flow.

The empirical law according to Poreh and Cermak, as formulated by Morkovin, of the normalized mean concentration profile recast as $\bar{c}/\bar{c}_w$ versus y/δ_π for the final mixing zone is adopted. Their scaling law for wall concentration ($\bar{c}_w$) is replaced by one based on the approximation $\overline{uc} \approx \bar{u}\,\bar{c}$ (partly justified by the work of Kibens and of Fiedler and Head) and the velocity defect law of Coles. The result, in reasonable agreement with the data of Poreh and Cermak, gives $U\delta_\pi \bar{c}_w/Q_i c_i$, $U\delta^* \bar{c}_w/Q_i c_i$, and $U\theta \bar{c}_w/Q_i c_i$ as slowly varying functions of U/u_τ. A noteworthy prediction is that c_Q, the ordinary boundary-layer volume-flux average concentration, is about $0.6\bar{c}_w$, so that c_Q, as an estimate of $\bar{c}_w$, is still about 40% low.

A comparison with preliminary data on mixing in an open-channel boundary layer injected with dyed water or dyed Polyox WSR-301 solution suggests that the

predictions of the negative roughness analogy are useful, at least in the case of low polymer concentration and moderate wall shear stress. Further comparison with more nearly two-dimensional mixing experiments are needed.

Appendix

VOLUME-FLUX AVERAGE CONCENTRATION

Following upon the definition of c_t in Eq. 9 in terms of Q_t, Eq. 4 and 10 yield

$$Q_i c_i / U\delta_\pi c_t = \int_0^\infty \gamma d\eta + (u_\tau/U)(1/k) \int_0^1 \gamma \ln \eta d\eta + (u_\tau/U)(\Pi/k) \int_0^1 \gamma(w-2)d\eta \qquad (21)$$

If $w \triangleq 2$ for $\eta > 1$, then Eq. 21 may be written as

$$Q_i c_i / U\delta_\pi c_t = [1 - (2\Pi/k)u_\tau/U] \int_0^\infty \gamma d\eta + (u_\tau/U)(1/k) \int_0^1 \gamma \ln \eta d\eta + (u_\tau/U)(\Pi/k) \int_0^\infty \gamma w(\eta) d\eta \qquad (22)$$

The three integrals can be evaluated if $\gamma(\eta)$ is known. There is a sizable amount of experimental information on $\gamma(x, y)$ in Newtonian-fluid boundary layers. Various investigators have found that their distributions can be described accurately in terms of two parameters, $\overline{Y}$ and σ, and the expression:

$$\gamma = \frac{1}{\sigma\sqrt{2\pi}} \int_y^\infty \exp\left[-\left(\frac{y-\overline{Y}}{\sigma\sqrt{2}}\right)^2\right] dy$$

$$= (1/2)\,\mathrm{erfc}\left(\frac{y-\overline{Y}}{\sigma\sqrt{2}}\right) \quad [\text{using } \mathrm{erf}(-a) \triangleq -\mathrm{erf}(a)] \qquad (23)$$

This relation has a simple, but not unique, interpretation: if for any given station x there is at every instant a single interface at $y = Y(x, t)$ between turbulent ($y < Y$) and irrotational flow, and if $Y(x, t)$ has a Gaussian probability density distribution with mean value $\overline{Y}$ and standard deviation σ, then the turbulence intermittency distribution $\gamma(x, y)$ is given by Eq. 23. γ equals 0.5 at $y = \overline{Y}$ and is essentially 1 for $y < \overline{Y} - 2.5\sigma$ and essentially 0 for $y > \overline{Y} + 2.5\sigma$. Fiedler and Head (Ref. 3) found in their experiments with both favorable and unfavorable pressure gradients that[6] $\overline{Y}/\delta$

[6] The meaning of δ in Ref. 3 is not defined but was assumed to be the 99% point in this work.

and σ/δ appeared to depend only on the profile form factor, $H \triangleq \delta^*/\theta$, and that there was no systematic effect of Reynolds number for the range covered, viz. $U\theta/\nu \approx 1000$ to 4000.

If this relation, that $\overline{Y}/\delta$ and σ/δ depend only on H, were exact, so that $\gamma = \gamma(\eta, H)$, it would mean that the intermittency in a constant-pressure boundary layer along a line of constant y/δ (or y/δ_π, to be precise) would vary with x as a result of the variation of H with U/u_τ. It seems, on the other hand, more reasonable that $\overline{Y}/\delta_\pi$ and σ/δ_π should be as nearly independent of x in a constant pressure, equilibrium flow as is the velocity-defect $(U - \bar{u})/u_\tau$ versus y/δ_π, since intermittency is primarily a property of the outer layer.

Several investigators have measured intermittency distributions in nearly constant-pressure flow and obtained very similar results. In particular, Coles (Ref. 8) reanalyzed Klebanoff's data (Ref. 18) and obtained $\overline{Y}/\delta_\pi = 0.825$ and $\sigma/\delta_\pi = 0.148$, after assuming $\Pi = 0.55$. The outer-layer similarity prediction is thus that $\overline{Y}/\delta_\pi = 0.825$ independent of U/u_τ. Figure 13 contrasts this prediction with the $\overline{Y}/\delta$ prediction from

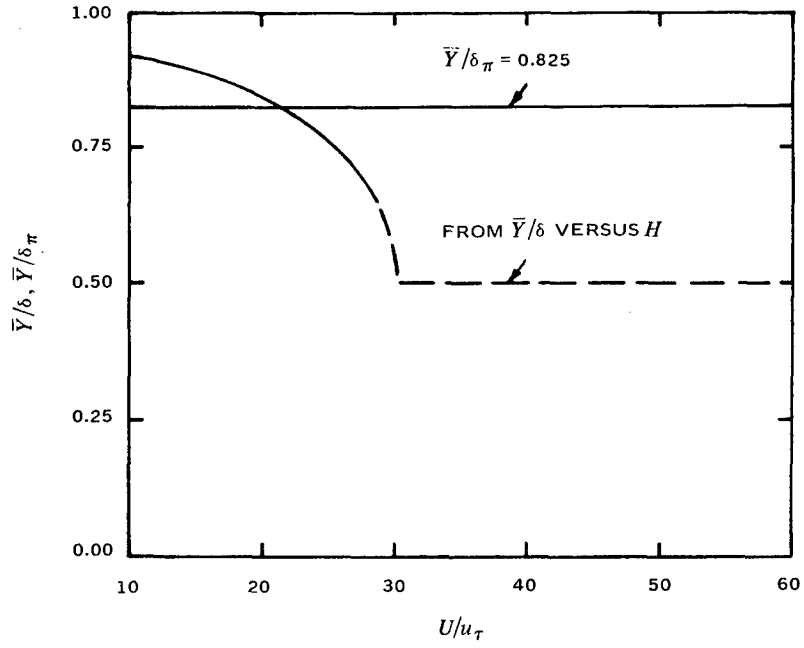

FIG. 13. Two Predictions for $\overline{Y}/\delta_\pi$ Versus U/u_τ for a Constant-Pressure Boundary Layer.

Ref. 3, combined with the well-known relation between H and U/u_τ for large boundary-layer Reynolds numbers:

$$H = (1 - Gu_\tau/U)^{-1}$$

$$G \triangleq \int_0^\infty [(U - \bar{u})/u_\tau]^2 \, d\eta \Big/ \int_0^1 (U - \bar{u})/u_\tau \, d\eta$$

$G = 6.64$ (as in Eq. 18)

(This value of G is quite reasonable, as can be seen in Ref. 4 and 14.)

Since the difference between δ_π and δ are only of the order of 10% for ordinary U/u_τ values, the disagreement in Fig. 13 cannot be attributed to that difference. The prediction based on the $\overline{Y}/\delta(H)$ relation of Ref. 3 clearly seems more suspect than the other because the experiments of Fiedler and Head for low H values were for very favorable pressure gradients. Thus the constant-$\overline{Y}/\delta_\pi$ behavior is assumed here.

Using $\overline{Y}/\delta_\pi = 0.825$ and $\sigma/\delta_\pi = 0.148$ and Eq. 23, the integrals in Eq. 22 can be evaluated. The first integral can be evaluated exactly:

$$\int_0^\infty \gamma d\eta = \gamma(0, \overline{Y}/\delta_\pi, \sigma/\delta_\pi)\overline{Y}/\delta_\pi + (\sigma/\delta_\pi \sqrt{2\pi}) \exp[-(\overline{Y}/\sigma\sqrt{2})^2]$$

For the assumed values of $\overline{Y}/\delta_\pi$ and σ/δ_π, a very good approximation is

$$\int_0^\infty \gamma d\eta \approx \overline{Y}/\delta_\pi$$

The second integral was evaluated numerically except for an interval containing the singularity in $\ln\eta$, which was handled analytically. The result is

$$\int_0^1 \gamma \ln\eta d\eta \approx -0.772\gamma(0, \overline{Y}/\delta_\pi, \sigma/\delta_\pi) - 0.198 \approx -0.970$$

Numerical integration of the third integral gives

$$\int_0^\infty \gamma w(\eta) d\eta \approx 0.668$$

These three results and $k = 0.41$ and $\Pi = 0.55$ in Eq. 22 yield the scaling law for c_t given in Eq. 11.

REFERENCES

1. Hoyt, J. W., and A. G. Fabula. "The Effect of Additives on Fluid Friction," presented at the Fifth Symposium on Naval Hydrodynamics, 10 to 12 September 1964, at Bergen, Norway. Washington, Department of the Navy (ONR ACR-112).

2. Naval Undersea Warfare Center. Attainable Friction Reduction on Long, Fast Vessels, by A. G. Fabula. Pasadena, Calif., NUWC, February 1969. (NUWC Technical Publication 123.)

3. Fiedler, H., and M. R. Head. "Intermittency Measurements in the Turbulent Boundary Layer," in J FLUID MECH, Vol. 25, No. 4 (1966), pp. 719-35.

4. Rotta, J. C. "Incompressible Turbulent Boundary Layers," in Mecanique de la Turbulence, Colloques Internationaux du Centre de la Recherche Scientifique, No. 108 (1962), pp. 255-85.

5. Granville, P. "The Frictionless Resistance and Velocity Similarity Laws of Drag-Reducing Polymer Solutions," in J SHIP RES, Vol. 12, No. 3 (September 1968), pp.201-212.

6. White, F. M. "An Analysis of Flat-Plate Drag With Polymer Additives," in J HYDRONAUT, Vol. 2, No. 4 (October 1968), pp. 181-6.

7. Clauser, F. H. The Turbulent Boundary Layer. Vol. IV, Advances in Applied Mechanics. New York, Academic Press, 1956. Pp. 2-51.

8. Coles, D. "The Law of the Wake in the Boundary Layer," in J FLUID MECH, Vol. 1, No. 2 (1956), pp. 191-226.

9. Johns Hopkins University. The Intermittent Region of a Turbulent Boundary Layer, by V. Kibens and S. G. Kovasznay. Baltimore, JHU, January 1969. (Report No. 1, Dept. Mech., DA-31-124-ARO-D-313).

10. Aeronautical Research Council. A New Two-Parameter Family of Mean Velocity Profiles for Incompressible Turbulent Boundary Layers on Smooth Walls, by B. G. J. Thompson. Great Britain, ARC, April 1965. (R. and M. 3463.)

11. Poreh, M., and J. E. Cermak. "Study of Diffusion From a Line Source in a Turbulent Boundary Layer," in INTERN J HEAT MASS TRANSFER, Vol. 7 (1964), pp. 1083–95.

12. Morkovin, M. V. "On Eddy Diffusivity, Quasi-Similarity, and Diffusion Experiments in Turbulent Boundary Layers," in INTERN J HEAT MASS TRANSFER, Vol. 8 (1965), pp. 129–45.

13. Schlichting, H. Boundary Layer Theory. New York, McGraw-Hill, 1960. 4th ed., p. 542.

14. Stanford University. An Experimental Study of Turbulent Boundary Layer on Rough Walls, by C. K. Liu, S. J. Kline, and J. P. Johnston. Stanford, Calif., S. U., July 1966. (Thermosciences Division, Department of Mechanical Engineering Report MD-15.)

15. Hydronautics, Inc. Experiments on Free Turbulence in Visco-Elastic Fluids, by J. Wu. Laurel, Md., Hydronautics, March 1965. (Technical Report 353-1.)

16. Hinze, J. O. Turbulence. New York, McGraw-Hill, 1959. P. 486.

17. Goren, Y., and J. F. Norbury. "Turbulent Flow of Dilute Aqueous Polymer Solutions," ASME TRANS, J BASIC ENG, Vol. 89, No. 4, Series D (December 1967), pp. 814–22.

18. National Advisory Committee on Aeronautics. Characteristics of Turbulence in a Boundary Layer With Zero Pressure Gradient, by P. S. Klebanoff. Washington, NACA, 1955. (NACA Report 1247.)

INITIAL DISTRIBUTION

1 Chief of Naval Material
2 Naval Air Systems Command
  NAIR-350
  NAIR-604
8 Naval Ordnance Systems Command
  NORD-03A
  NORD-035
  NORD-05
  NORD-05121
  NORD-052
  NORD-054
  NORD-054131
  NORD-9132
3 Naval Ship Engineering Center
  NSEC-6103E
  NSEC-6136B (F. S. Cauldwell)
  NSEC-6141 (J. E. M. Coleman)
6 Naval Ship Systems Command
  NSHP-034
  NSHP-0341
  NSHP-0342
  NSHP-037C
  NSHP-0372
  NSHP-205
2 Office of Naval Research
  ONR-438
  ONR-466
3 Anti-Submarine Warfare Systems Project Office (ASW-13, 14, 20)
2 Naval Academy
  Library
  Prof. Bruce Johnson
1 Naval Air Development Center, Johnsville
1 Naval Electronics Laboratory Center
1 Naval Ordnance Laboratory, White Oak
1 Naval Personnel Research and Development Laboratory
3 Naval Postgraduate School, Monterey
  Library, Technical Reports Section
  Prof. J. V. Sanders
  Prof. T. Sarpkaya

2 Naval Research Laboratory
Library
Dr. R. C. Little
1 Naval Ship Research and Development Center, Annapolis Division
5 Naval Ship Research and Development Center, Carderock Division
Library (1)
Code 508 (2)
Code 580 (1)
Code 581 (1)
1 Naval Ship Research and Development Laboratory, Panama City
2 Naval Torpedo Station, Keyport
Quality Evaluation Laboratory, Technical Library
Director, Research and Engineering
3 Naval Underwater Weapons Research and Engineering Station
Library
J. F. Brady
R. J. Grady
1 Naval Weapons Center (Code 753)
1 Naval Weapons Services Office (Code DM)
2 Navy Underwater Sound Laboratory, Fort Trumbull
Dr. H. P. Bakewell, Jr.
Dr. H. H. Schloemer
20 Defense Documentation Center
1 Applied Physics Laboratory, University of Washington
1 Bolt Beranek and Newman, Inc. (D. M. Chase)
2 Colorado State University
Prof. J. E. Cermak, College of Engineering
Prof. J. P. Tullis, Dept. of Civil Engineering
1 General Electric Co., Mechanical Engineering Laboratory (W. B. Giles)
1 Hydronautics, Inc. (M. P. Tulin)
1 Illinois Institute of Technology (Prof. M. V. Morkovin)
1 Iowa Institute of Hydraulic Research, University of Iowa (Prof. L. Landweber)
1 The Johns Hopkins University, Department of Mechanics (Prof.L.S.G.Kovasznay)
1 LTV Research Center, Dallas (Dr. C. S. Wells, Jr.)
1 Oceanics, Inc. (Dr. P. Kaplan)
1 Ordnance Research Laboratory, Pennsylvania State University
1 Pennsylvania State University, Department of Aerospace Engineering
(Prof. J. L. Lumley)
1 Purdue University, School of Mechanical Engineering (Prof. A. T. McDonald)
1 Socony Mobil Oil Co., Field Research Laboratory, Dallas (G. Savins)
1 St. Anthony Falls Hydraulic Laboratory, University of Minnesota
(Prof. J. M. Wetzel)
1 Stanford University, Mechanical Engineering Department
(Prof. S. J. Kline)
1 The University of Arizona, College of Engineering (Prof. D. M. McEligot)
1 University of California, San Diego (Prof. C. H. Gibson)

UNCLASSIFIED

Security Classification

DOCUMENT CONTROL DATA - R & D

(Security classification of title, body of abstract and indexing annotation must be entered when the overall report is classified)

1. ORIGINATING ACTIVITY *(Corporate author)*
Naval Undersea Research and Development Center
San Diego, Calif. 92132

2a. REPORT SECURITY CLASSIFICATION
UNCLASSIFIED

2b. GROUP

3. REPORT TITLE
DILUTION IN A TURBULENT BOUNDARY LAYER WITH POLYMERIC FRICTION REDUCTION

4. DESCRIPTIVE NOTES *(Type of report and inclusive dates)*
Mathematical analysis helpful in planning friction reduction system

5. AUTHOR(S) *(First name, middle initial, last name)*
A. G. Fabula, T. J. Burns

6. REPORT DATE	7a. TOTAL NO. OF PAGES	7b. NO. OF REFS
April 1970	26	18

8a. CONTRACT OR GRANT NO.	9a. ORIGINATOR'S REPORT NUMBER(S)
b. PROJECT NO. ORD-054-000/200-1/R 109-01-03	NUC TP 171
c.	9b. OTHER REPORT NO(S) *(Any other numbers that may be assigned this report)*
d.	

10. DISTRIBUTION STATEMENT This document is subject to special export controls and each transmittal to foreign nationals may be made only with the prior approval of the Naval Undersea Research and Development Center.

11. SUPPLEMENTARY NOTES	12. SPONSORING MILITARY ACTIVITY
	Naval Ordnance Systems Command Washington, D.C. 20360

13. ABSTRACT

The dilution by turbulent mixing of a polymer solution after injection into a turbulent boundary layer with polymeric friction reduction is considered. Two-dimensionality and constant-pressure flow over a flat plate are assumed. The intermittency of turbulence and scalar concentration, as well as the effects of friction-reduction on the mean velocity profile, are treated. The "negative roughness" analogy of polymeric friction reduction is invoked to justify the assumption that all significant properties of the outer-layer region satisfy the Newtonian-fluid outer-layer similarity laws, including those for velocity-defect, turbulence intermittency, and mean concentration in the final zone of mixing. (This assumption is expected to be valid in cases of low polymer concentration and moderate wall shear stresses.) Thus the polymer is treated like a passive scalar in the outer layer. A notable feature of the predicted mixing similarity law is that the mean concentration near the wall is underestimated by about 40% by the ordinary volume-flux average concentration in the boundary layer.

A comparison with preliminary experimental results suggests that the predictions of far-downstream mixing are useful at least for low polymer concentrations and moderate wall shear stresses.

The final-zone predictions are expected to be useful in estimating the obtainable friction reduction and boundary layer development on a slender body far downstream of a slot through which polymer solution is injected into the boundary layer. How close to an injection slot these relations are useful, and where and how the concentration fluctuations about the mean must be considered, remain to be investigated.

14. KEY WORDS	LINK A		LINK B		LINK C	
	ROLE	WT	ROLE	WT	ROLE	WT
Turbulent boundary-layer mixing (diffusion; dilution)						
Polymeric friction reduction						
Toms effect						
"Negative Roughness" analogy						
Boundary-layer injection						

1 University of Rhode Island, Department of Mechanical and Ocean Engineering (Prof. F. M. White)
1 University of Southern California, Department of Aerospace Engineering (Prof. R. E. Kaplan)
1 The University of Tennessee Space Institute (Prof. J. R. Maus)

Center Distribution

05
14 (T. G. Lang, H. V. L. Patrick)
131
133 (2)
25
2501
254
25402
25403
2541
2541 (T. J. Burns)
2542
2542 (S. J. Barker, D. M. Nelson)
2543
96